

Maximally Flat and Least-Square Co-Design of Variable Fractional Delay Filters for Wideband Software-Defined Radio*

Haolin Li[†], Joris Van Kerrebrouck[‡], Johan Bauwelinck[§],
Piet Demeester[¶] and Guy Torfs^{||}

*Department of Information Technology, IDLab,
Ghent University-imec,
Ghent 9000, Belgium*
[†]haolin.li@ugent.be

[‡]joris.vankerrebrouck@ugent.be

[§]johan.bauwelinck@ugent.be

[¶]piet.demeester@ugent.be

^{||}guy.torfs@ugent.be

Received 24 October 2017

Accepted 16 March 2018

Published 9 April 2018

This paper describes improvements in a Farrow-structured variable fractional delay (FD) Lagrange filter for all-pass FD interpolation. The main idea is to integrate the truncated *sinc* into the Farrow structure of a Lagrange filter, in order that a superior FD approximation in the least-square sense can be achieved. Its primary advantages are the lower level of mean-square-error (MSE) over the whole FD range and the reduced implementation cost. Extra design parameters are introduced for making the trade-off between MSE and maximal flatness under different design requirements. Design examples are included, illustrating an MSE reduction of 50% compared to a classical Farrow-structured Lagrange interpolator while the implementation cost is reduced. This improved variable FD interpolation system is suitable for many applications, such as sample rate conversion, digital beamforming and timing synchronization in wideband software-defined radio (SDR) communications.

Keywords: Canonical signed digit (CSD); Farrow structure (FS); FPGA; fractional delay (FD); Lagrange; least-square (LS); mean-square-error (MSE).

1. Introduction

Fractional delay (FD) filtering is utilized in many applications of signal processing, such as timing mismatch calibration of time-interleaved analog-to-digital converters (ADCs),¹⁻³ sample rate conversion,⁴ image processing,⁵ digital beamforming⁶ and

*This paper was recommended by Regional Editor Piero Malcovati.

[†] Corresponding author.

timing synchronization in digital receivers.⁷ Specifically, in digital communication systems, the propagation delay from the transmitter to the receiver is generally unknown at the receiver. Hence, symbol timing must be derived from the received signal. When designing a digital baseband receiver on field programmable gate arrays (FPGAs), the received signal is typically uniform-sampled at a fixed ADC clock. Thus, the timing error is a fraction of the ADC sample period and can vary with time. This timing error can significantly degrade the communication, thus, timing adjustment must be done before decoding the received signal.

Variable FD interpolation filters have been widely investigated for timing synchronization in all-digital receivers since it is desired to realize the fractional interpolation in an efficient way from the perspective of hardware implementation.^{7,8} The well-known Farrow structure (FS) can easily accommodate adjustable FDs without the need of changing the filter coefficients,^{9–14} and hence its constant filter coefficients can be efficiently realized in sum-of-power-of-two (SPT) representation¹⁵ or even in canonical signed digit (CSD) representation¹⁶ on FPGA. Generally, digital filters are usually divided into two classes: finite impulse response (FIR) filters and infinite impulse response (IIR) filters. The Thiran all-pass filter is one of the most popular IIR FD filters, however, pipelining is not allowed owing to the inherent feedback loop, limiting the maximal clock frequency of the FD interpolation systems. In contrast to an IIR filter, there is no feedback in an FIR filter, making it inherently stable. The FIR filters implemented on FPGA usually use a series of delays, multipliers and adders to generate the filter outputs. Therefore, an FIR filter can be easily pipelined to increase the maximal clock frequency, and the effective throughput and the clock frequency are decoupled thanks to parallelization. The maximally allowable clock frequency of an FIR filter is then limited to the speed of the FPGA building blocks. In this sense, the FIR-based variable FD interpolation with FS-pipelined structure is preferred when implementing a wideband all-digital receiver system on FPGA. In Ref. 17, a multi-rate technique has been applied to the design of wideband variable FD FIR filters by making the input signal narrowband with respect to the filter sampling rate. However, increasing the sampling rate before the FS would increase the resources for a given maximal clock frequency in FPGA parallelization. Moreover, in all-digital receiver systems, the Shannon sampling scheme is usually implemented by using one ADC. In this case, the wideband FD interpolation filter using the derivative sampling method¹⁸ is only applicable with a discrete-time differentiator on FPGA, leading to extra implementation cost.

Variable FD interpolation filters are required to have a constant magnitude response for any given FD delays. The weighted-least-square (WLS) or least-square (LS),^{19–23} minimax²⁴ and maximally flat^{25,26} criteria can be used for the approximation of these FD filters as discussed in Ref. 27. The WLS (or LS) method is a closed-form design. Since the filter coefficients are obtained by minimizing the energy of the weighted error between the actual transfer characteristic and the desired transfer characteristic, this design method can provide us with an optimal solution in

the sense of LS error. The maximally flat approximation leads to the closed-form solution of FD FIR filters with a maximally flat magnitude response of unity and a constant group delay response at the zero frequency. The maximally flat FIR FD interpolation systems, also known as the Lagrange-type FD interpolation filters, are easy to use because its coefficients can be explicitly expressed as polynomials of the variable FD parameter. Different formulas for the Lagrange interpolators are derived in Ref. 25. It has been also shown that truncating the coefficients can also obtain a variable FD filter with wider bandwidth as compared with the original one (without truncation).²⁸ However, the approximation of Lagrange FD interpolation filters is heavily degraded at high frequencies, especially when the FD approaches half the sample period.

In this paper, we will combine both the maximally flat and the LS (or WLS) criteria to optimize the FD interpolation filters. Our observations show that if the sub-filters of an FS-based Lagrange interpolation are slightly modified by introducing extra correction terms derived from the LS design method, a superior approximation of an ideal FD interpolation can be obtained without additional implementation cost. The polynomial degree, the filter order and the length and location of the correction terms can be further jointly optimized. The contribution of this paper is three-fold. First, the variable FD interpolation filter approaches the optimal solution in the LS error sense. Second, extra design parameters are provided to make the trade-off between the LS error and the maximal flatness for different design requirements. Third, the proposed filter features the advantages of the FS in terms of variable FD.

The remainder of this paper is organized as follows. In Sec. 2, the LS design method, the FS-based variable FD FIR filter and the Lagrange interpolation are reviewed. In this section, performance metrics are defined as well. In Sec. 3, the cascaded filter structure and its dual form are described. In Sec. 4, the LS-based interpolation filter is integrated into the FS of the Lagrange variable FD interpolation filter. The performance and the implementation cost of the proposed filter are evaluated. Finally, conclusions are drawn in Sec. 5.

2. FD Interpolation

This section recapitulates the theory of the FD interpolation and reviews the properties of a truncated *sinc*, the FS, and Lagrange interpolation filters.

2.1. LS sinc interpolation

The ideal frequency response of a variable FD filter is given by

$$\begin{aligned} H_{\text{ideal}}(e^{j\omega T_s}) &= e^{-j\omega DT_s} \\ &= e^{-j\omega(D_{\text{int}}+d)T_s}, \end{aligned} \quad (1)$$

where T_s is the sample period and D is a positive real number that indicates the total delay in number of samples of the digital FIR filter impulse response with $D = D_{\text{int}} + d$. D_{int} generally represents the integer delay throughout this paper (D_{int} will vary for different filter lengths) and d is the fractional part of the delay in the desired range $[0,1]$. $\omega \in [0, \omega_p]$ is the normalized angular frequency and ω_p is a parameter defining the passband edge frequency, $\omega_p \leq \pi$. The ideal frequency response of an all-pass FD interpolation filter specified by $\omega_p = \pi$ corresponds to the *sinc* impulse response expressed as

$$h_{\text{ideal}}(n) = \text{sinc}(n - D), \quad n = 0, 1, 2, \dots \quad (2)$$

This is an IIR digital filter with no recursive form and hence unrealizable. The frequency response of the FIR filter used to approximate the ideal frequency response is given by

$$\hat{H}(e^{j\omega T_s}) = \sum_{n=0}^N \hat{h}(n) e^{-j\omega n T_s}. \quad (3)$$

The frequency response error $E(\omega)$ is defined as the difference between ideal frequency response and the approximated frequency response.

$$E(\omega) = H_{\text{ideal}}(e^{j\omega T_s}) - \hat{H}(e^{j\omega T_s}). \quad (4)$$

The filter coefficient $\hat{h}(n)$ is determined by minimizing the following error function:

$$\begin{aligned} J(\hat{h}) &= \frac{T_s}{2\pi} \int_{-\pi/T_s}^{\pi/T_s} W(\omega) |E(\omega)|^2 d\omega \\ &= \frac{T_s}{2\pi} \int_{-\pi/T_s}^{\pi/T_s} W(\omega) |H_{\text{ideal}}(e^{j\omega T_s}) - \hat{H}(e^{j\omega T_s})|^2 d\omega, \end{aligned} \quad (5)$$

where $W(\omega)$ is a nonnegative weighting function. We assume a uniform weighting function over the entire frequency band (all-pass case) throughout this paper. According to *Parseval's* theorem, the error function can be rewritten as follows:

$$J(\hat{h}) = \sum_{n=0}^{\infty} |h_{\text{ideal}}(n) - \hat{h}(n)|^2. \quad (6)$$

The optimal $\hat{h}(n)$ in LS sense for a given FD d and filter order N is expressed in Eq. (7). Note that for variable FDs, a new set of filter coefficients should be computed for each delay. However, for a given d , this optimal solution will outperform the solution found by minimizing the error function over both the entire frequency range and the entire FD range:

$$\hat{h}(n) = \begin{cases} \text{sinc}(n - D), & 0 \leq n \leq N, \\ 0, & \text{otherwise.} \end{cases} \quad (7)$$

2.2. Farrow structure

Farrow suggested that every filter coefficient of an FIR FD filter could be expressed as an M th-order polynomial in the variable delay parameter d .^{10,29} The FS consists of a set of constant coefficient filters called sub-filters, and the outputs of the sub-filters are multiplied by different powers of the variable FD parameter and then added together to form the ultimate output of the variable FD interpolation. The general FS is presented in Fig. 1, where $C_m(z)$ denotes the Z -transform frequency response of the m th FS sub-filter. The ideal filter response in Eq. (1) can be approximated using the FS with the following frequency response:

$$H_d(z) = \sum_{m=0}^M C_m(z)d^m. \tag{8}$$

The fixed FIR sub-filters $C_m(z)$ approximate k th-order differentiators with frequency responses given as follows:

$$C_m(z) \approx \frac{(-j\omega T_s)^m}{m!} e^{-j\omega D_{\text{int}} T_s}, \quad 0 \leq m \leq M, \tag{9}$$

which is obtained by truncating the Taylor series expansion of Eq. (1). In the FS, each sub-filter is an N th-order FIR filter as depicted in Fig. 2 and its Z -transform frequency response is defined as

$$C_m(z) = \sum_{n=0}^N C_m(n)z^{-n}, \quad 0 \leq m \leq M, \tag{10}$$

where $C_m(n)$ denotes the n th coefficient of the m th sub-filter. The coefficient matrix is given as follows:

$$C = \begin{pmatrix} C_M(N) & \cdots & C_1(N) & C_0(N) \\ C_M(N-1) & \cdots & C_1(N-1) & C_0(N-1) \\ \vdots & \ddots & \vdots & \vdots \\ C_M(0) & \cdots & C_1(0) & C_0(0) \end{pmatrix}. \tag{11}$$

In particular, the first sub-filter has an all-pass filtering characteristic with a unit pulse given by

$$\begin{aligned} C_0(z) &= e^{-j\omega D_{\text{int}} T_s}, \\ C_0(n) &= \delta(n). \end{aligned} \tag{12}$$

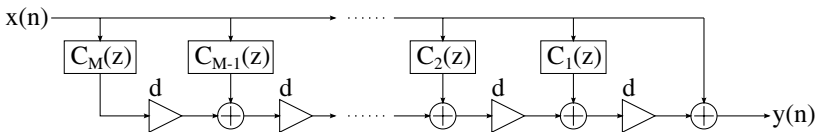


Fig. 1. The general FS with adjustable FD d and $C_0(z) = 1$.

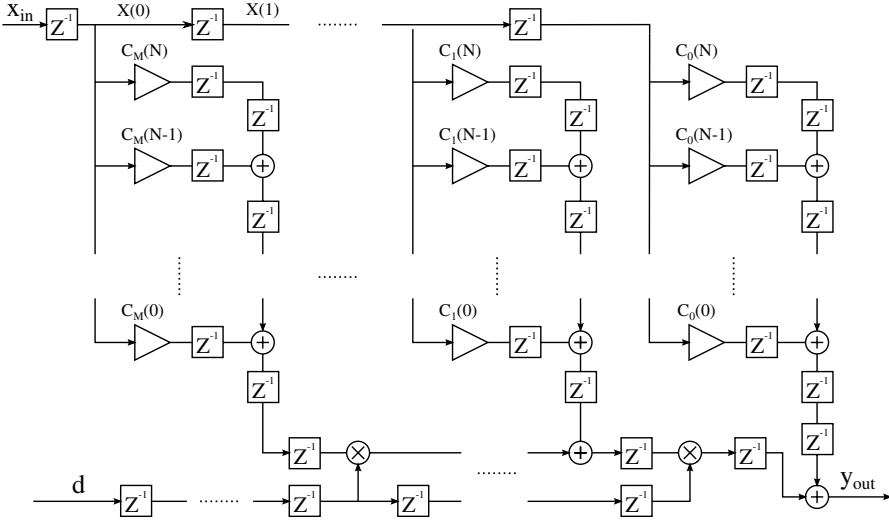


Fig. 2. The pipelined FS for a polynomial-based Lagrange interpolation filter, and this structure works for both even and odd orders.

The differentiators are realized by making $C_m(n)$ symmetrical or anti-symmetrical for even or odd n , which is also beneficial in terms of implementation complexity. The impulse response of the FS is expressed as

$$h_d(n) = \sum_{m=0}^M C_m(n)d^m, \quad 0 \leq n \leq N. \tag{13}$$

The main advantage of the FS is that all sub-filter coefficients are fixed, the only changeable parameter is the FD d , which leads to a less computation intensive implementation. The whole filter structure is pipelined in Fig. 2 to lower the computation intensity during a single clock cycle, therefore allowing the increase of the maximal clock frequency.

2.3. Lagrange interpolation

The Lagrange interpolator is also known as a maximally flat FIR fractional-sample delay system, meaning that all the derivative terms in the Taylor series expansion of the frequency response error are zeroed around dc ($z = 1$). Therefore, the Lagrange interpolation is very accurate at low frequencies and is a widely used method in signal processing algorithms. The coefficients of an N th-order Lagrange interpolator for FD can be expressed in the following way:

$$h_L(n) = \prod_{\substack{k=0 \\ k \neq n}}^N \frac{D - k}{n - k}, \quad 0 \leq n \leq N. \tag{14}$$

From the Lagrange interpolation formula, the output of the Lagrange interpolation is the delayed input sample for an integer delay D , i.e., no approximation error is made in this case. The coefficient $C_m(n)$ of the Farrow-structured Lagrange interpolator can be obtained from the inverse of the $N \times N$ Vandermonde matrix V^{-1} , where each row represents the sub-filter $C_m(z)$.

We can compute the value of the magnitude response of the Lagrange interpolator at $\omega = \pi$. This value is not equal to unity except for some very special cases (when the FD is zero). The overall magnitude response deviates from the ideal magnitude of unity as the normalized angular frequency ω moves away from the zero frequency and approaches π . This deviation becomes even worse when the FD approaches 0.5, the worst case. The truncated Lagrange interpolator can be introduced to mitigate the magnitude response deviation at high frequencies by sacrificing passband flatness.²⁸

2.4. Performance metrics

To compare the FD approximation of different interpolation filters, the frequency response error and the MSE are evaluated as performance metrics. The frequency response error is defined in Eq. (4) and the MSE is defined as

$$\text{MSE} = \frac{1}{N_1} \sum_{i=1}^{N_1} (Y_i - \hat{Y}_i)^2, \tag{15}$$

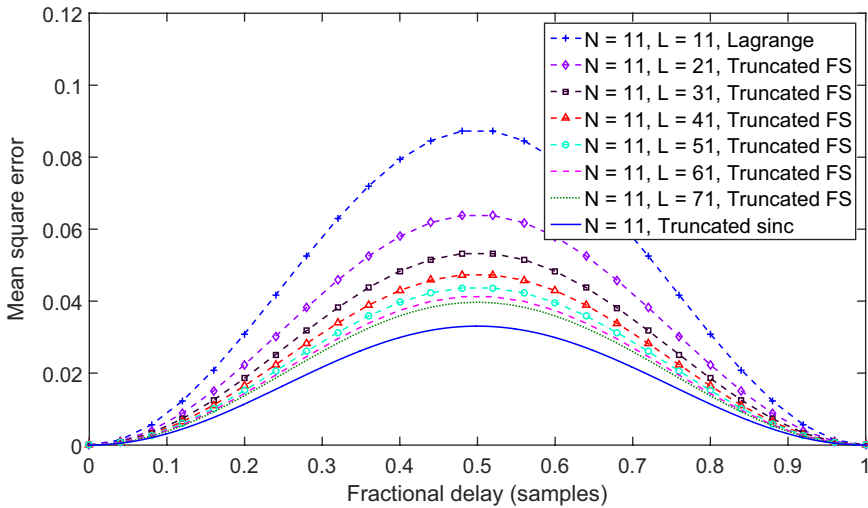


Fig. 3. MSE curves of truncated Lagrange interpolation filters of order N and different prototype filter orders L using the FS.

where N_1 is the number of samples, \hat{Y}_i and Y_i are the interpolated sample and the ideal sample with normalized power, respectively. The MSE of the truncated Lagrange interpolator increases when d approaches 0.5, as presented in Fig. 3. L represents the prototype filter order described in Ref. 28.

3. Combined Filter Structure

As described in Ref. 30, to compensate the degradation of the Lagrange interpolation at $d = 0.5$ and obtain a low level of MSE over the whole range of d , a cascaded *sinc*-Farrow filter structure is first introduced. The block diagram of this cascaded filter structure is depicted in Fig. 4. Once the variable delay d approaches 0.5, the branch $H_1(z)$ becomes active and the new FD ($d - 0.5$) is fed to the FS. The $H_0(z)$ and $H_1(z)$ represent the frequency response of the truncated *sinc* at $d = 0$ and $d = 0.5$, respectively.

As shown in Fig. 5, at $d = 0.5$, the MSE of the cascaded *sinc*-Farrow filter exhibits a minimal value that is mainly determined by the order of the *sinc* interpolation filter ($H_0(z)$ and $H_1(z)$ have the same filter order N as the FS), because, as presented in Fig. 3, there is no MSE caused by the Lagrange interpolation at $d = 0$. By properly switching the outputs between these two filter branches, the overall MSE can be reduced. The active ranges of $H_1(z)$ are indicated in Fig. 5, which are determined by the MSE values of the cascaded interpolation filters $H_0(z)H_d(z)$ and $H_1(z)H_d(z)$.

Note that the first sub-filter $C_0(z)$ is equal to 1 for all delay values in FS, as presented in Fig. 1 and Eq. (12). Thus, the dual form of the cascaded filter structure, i.e., Farrow-*sinc* can be used and the first sub-filter $C_0(z)$ can be substituted by $H_1(z)$ without having to change the parameter d .³⁰

The orders of the FS and $H_1(z)$ are first kept equal for simplicity. The delay line represented by $H_0(z)$ is inherently included in the pipelined structure (referred to Fig. 2). When the FD d approaches 0.5, the deviation $\Delta h(n)$ of the Lagrange interpolation from the *sinc*-interpolation (both filters at $d = 0.5$) is added to the column $C_0(n)$ of the FS $(N + 1) \times (M + 1)$ coefficient matrix. This yields a new column $C'_0(n)$. Thus, when d approaches 0.5, the coefficients should be switched from $C_0(n)$ to $C'_0(n)$ and the update of the FD to $(d - 0.5)$ is no longer required. The calculation

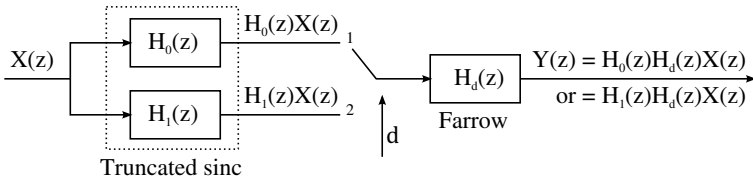


Fig. 4. The cascaded *sinc*-Farrow filter structure.

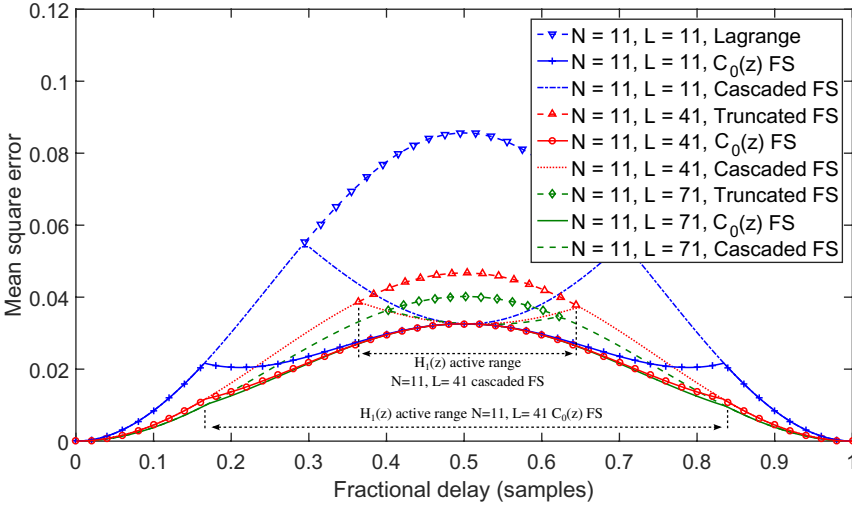


Fig. 5. MSE curves of combined Farrow filter structure of order $N = 11$ and $K = 0$.

for $C'_0(n)$ is expressed as follows:

$$\Delta h(n) = \text{sinc}(n - D_{\text{int}} - d)|_{d=0.5} - h_{d=0.5}(n), \quad (16)$$

$$C'_0(n) = C_0(n) + \Delta h(n), \quad 0 \leq n \leq N, \quad (17)$$

where $h_{d=0.5}(n)$ is the Farrow-structured Lagrange FD interpolation filter at $d = 0.5$ (referred to Eq. (13)) and $C_0(n)$ is the time-domain impulse response of the sub-filter $C_0(z)$ (referred to Eq. (12)).

It is easily noted that this Farrow-*sinc* filter bank structure (denoted as “ $C_0(z)$ FS” in Fig. 5) has the same MSE value as the cascaded *sinc*-Farrow filter structure at $d = 0.5$. However, the remarkable aspect of this Farrow-*sinc* structure is that the MSE value starts decreasing when d deviates from 0.5 as illustrated in Fig. 5 because the remaining sub-filters of FS compensate the FD approximation error. Therefore, the useful delay range between the two intercept points is widened compared to the cascaded *sinc*-FS at the same implementation complexity. It should be pointed out that the Lagrange filter has good FD approximation when d is far from 0.5, even for low filter orders. This allows us to jointly optimize the order of the Farrow-structured Lagrange filter and $H_1(z)$ in order to achieve a superior performance. The design procedure is slightly modified for the joint optimization. Assuming that the order of $H_1(z)$ is now $N + 2K$. The FS of order N is first truncated from the prototype FS of order L . Second, the Farrow $(N + 1) \times (M + 1)$ coefficient matrix is extended to a $(N + 1 + 2K) \times (M + 1)$ matrix by adding K zeros above and below the original Farrow coefficient matrix, which is nothing else than pipelining the signal. Hence, Eqs. (16) and (17) are again applicable. The obtained coefficient matrix is

expressed as follows:

$$C' = \begin{pmatrix} 0 & \cdots & 0 & \Delta h(N + 2K) \\ \vdots & \ddots & \vdots & \vdots \\ 0 & \cdots & 0 & \Delta h(N + K + 1) \\ C_M(N) & \cdots & C_1(N) & C_0(N) + \Delta h(N + K) \\ C_M(N - 1) & \cdots & C_1(N - 1) & C_0(N - 1) + \Delta h(N + K - 1) \\ \vdots & \ddots & \vdots & \vdots \\ C_M(0) & \cdots & C_1(0) & C_0(0) + \Delta h(K) \\ 0 & \cdots & 0 & \Delta h(K - 1) \\ \vdots & \ddots & \vdots & \vdots \\ 0 & \cdots & 0 & \Delta h(0) \end{pmatrix}. \quad (18)$$

The optimization map for different orders of Farrow-structured Lagrange filters and $H_1(z)$ filters with $L = N + 30$ is shown in Fig. 6 where the optimal filter orders can be chosen for a given MSE performance requirement. In addition, this optimization map reveals that Lagrange interpolation performance only increases slightly with increasing filter order, while the order of $H_1(z)$ has significant influence.

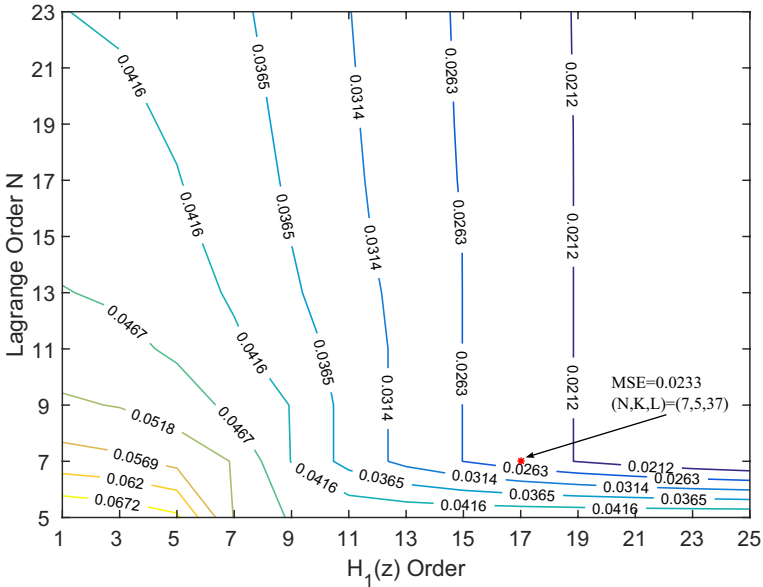


Fig. 6. Optimization map showing MSE performance with different orders of Lagrange and $H_1(z)$ filters. The values represent the worst MSEs over the whole FD range when the corresponding Lagrange and $H_1(z)$ filter orders are used in the combined filter structure “ $C_0(z)$ FS”.

An example of optimal filter orders is indicated on the optimization map. The main advantage of using the combined filter structure lies in the fact that, when jointly optimizing the two filtering blocks, the computational complexity to generate practically the same filtering performance can be drastically decreased.

4. Proposed Interpolation Filter

In this section, we propose a design technique in which the overall filter $H_d(z)$ of FS is modified to improve the FD interpolation at $d = 0.5$. This technique is based on the Farrow-structured Lagrange interpolation (maximally flat) and the truncated *sinc* (optimal in LS error for a given d , filter order N and $\omega_p = \pi$).

4.1. Desired interpolation properties

Both the truncated *sinc* and the Lagrange interpolation are very accurate when the FD delay d equals 0 or 1. Because the output of the Lagrange interpolation at integer delays is the delayed discrete input sample itself, no FD approximation error is made in this case. This high accuracy at integer delays should be preserved in the interpolation filter design.

As expressed in Eq. (12), the first sub-filter $C_0(z)$ possesses the all-pass transfer characteristic (i.e., its cut-off frequency exactly equals π). Further, note that in Eq. (8), the sub-filter $C_m(z)$ is weighted with d^m . Since d is limited in the FD range $[0, 1]$, the contribution of $C_m(z)$ for $1 \leq m \leq M$ to the overall transfer function is certainly less than that of $C_0(z)$. Moreover, the greater the sub-filter index m is, the less the influence of $C_m(z)$ is. Thus, it is preferred for wideband interpolation design that the correction term $\Delta h(n)$ is introduced in other sub-filters instead of $C_0(z)$.

As discussed in Sec. 2.1, in the LS error sense, the truncated *sinc* is optimal over the entire band $0 \leq \omega \leq \pi$ for a given FD d and FIR filter order N . It is also desirable to achieve these optimal LS errors for variable FD d with a single FS.

4.2. Maximally flat and LS co-design

Because the first two design considerations in Sec. 4.1 are the properties of the FS-based Lagrange interpolation, we first improve the FD interpolation performance at $d = 0.5$ in the LS error sense. The correction term for the chosen index m_1 and corresponding sub-filter $C_{m_1}(z)$ should be adapted as follows:

$$\begin{aligned} \Delta h_{d=0.5}(n) &= \text{sinc}(n - D_{\text{int}} - d)|_{d=0.5} - h_{d=0.5}(n), \\ \Delta h_{m_1}(n) &= \left. \frac{\Delta h_{d=0.5}(n)}{d^{m_1}} \right|_{d=0.5}, \\ C'_{m_1}(n) &= C_{m_1}(n) + \Delta h_{m_1}(n), \quad 0 \leq n \leq N, \\ W_{\Delta h}(m_1, d) &= \left(\frac{d}{0.5} \right)^{m_1}, \quad 1 \leq m_1 < M, \end{aligned} \tag{19}$$

where $\Delta h_{d=0.5}(n)$ is the deviation of the Lagrange interpolation from the truncated *sinc* at $d = 0.5$. $W_{\Delta h}(m_1, d)$ is the weight function of $\Delta h_{d=0.5}(n)$ in the overall impulse response. $\Delta h_{m_1}(n)$ is the correction term which should be adapted for the new sub-filter impulse response $C'_{m_1}(n)$. When d decreases from 0.5 to 0, the weight of $\Delta h_{d=0.5}(n)$ starts decreasing accordingly. In this way, the contribution of $\Delta h_{d=0.5}(n)$ to the overall impulse response becomes lower. This contribution will even vanish rapidly when the sub-filter index m_1 is large. Moreover, for $d = 0$, this correction term has no more influence, regardless of the chosen sub-filter index m_1 , and the output of the interpolator is then the delayed input sample itself. As discussed before, no approximation error is made at $d = 0$ thanks to the all-pass characteristic of $C_0(z)$. Denote the new equivalent impulse response as $h'_d(n)$ that is obtained by applying the new coefficient matrix denoted as $C'_m(n)$ to Eq. (13).

However, when d increases from 0.5 to 1, the weight increases exponentially, leading to a large approximation error. The same approach can be applied to improve the interpolation at an intermediate FD delay of, e.g., $d = 0.8$. Attention should be paid when choosing the second sub-filter index m_2 . m_2 should be greater than m_1 , otherwise, the improvement of the FD approximation at $d = 0.5$ will be contaminated. The second correction term is calculated based on the previous modified impulse response $h'_d(n)$ and the truncated *sinc* at $d = 0.8$. Denote now the new obtained impulse response and the new coefficient matrix as $h''_d(n)$ and $C''_m(n)$, respectively:

$$\begin{aligned} \Delta h_{d=0.8}(n) &= \text{sinc}(n - D_{\text{int}} - d)|_{d=0.8} - h'_{d=0.8}(n) \\ &= \text{sinc}(n - D_{\text{int}} - d)|_{d=0.8} - h_{d=0.8}(n) \\ &\quad - \Delta h_{d=0.5}(n)W_{\Delta h}(m_1, d = 0.8), \end{aligned} \tag{20}$$

$$\Delta h_{m_2}(n) = \left. \frac{\Delta h_{d=0.8}(n)}{d^{m_2}} \right|_{d=0.8},$$

$$C''_{m_2}(n) = C'_{m_2}(n) + \Delta h_{m_2}(n), \quad 0 \leq n \leq N, \tag{21}$$

$$W_{\Delta h}(m_2, d) = \left(\frac{d}{0.8} \right)^{m_2}, \quad m_1 < m_2 < M.$$

Due to the introduction of these extra correction terms, the output of the FD interpolation at $d = 1$ is no longer the delayed input sample. This approximation error can be further compensated by introducing the third correction term for the FD interpolation at $d = 1$. We choose the third sub-filter index $m_3 = M$ so that this correction term has the least influence on the previous correction terms while maintaining zero approximation error at $d = 1$. As described in Sec. 3, the filter orders and the length of the correction terms can be optimized. A similar coefficient

matrix as Eq. (18) can be obtained for this proposed filter structure:

$$\begin{aligned} \Delta h_{d=1}(n) &= \text{sinc}(n - D_{\text{int}}) - h''_{d=1}(n), \\ \Delta h_{m_3}(n) &= \left. \frac{\Delta h_{d=1}(n)}{d^{m_3}} \right|_{d=1}, \\ C'''_{m_3}(n) &= C''_{m_3}(n) + \Delta h_{m_3}(n), \quad 0 \leq n \leq N, \\ W_{\Delta h}(m_3, d) &= \left(\frac{d}{1}\right)^{m_3}, \quad m_3 = M. \end{aligned} \tag{22}$$

4.3. Performance evaluation

As shown in Fig. 7, compared to the MSE values of the combined filters (cascaded or “ $C_0(z)$ FS”), the MSE of the proposed filter is lower when d is approaching the integer delays. For $L = 11$, the MSE curve round $d = 0.5$ is slightly tilted from that of a truncated sinc due to the introduction of the second and third correction terms. For $L = 41$, this difference becomes negligible. This design technique removes the requirement of switching between different filters required by combined filters as discussed in Sec. 3. The corresponding frequency response errors are depicted in Fig. 8. Note that, the passband ripples of the truncated Lagrange, truncated sinc , and proposed interpolation filters are less when d is closer to integer delays as shown in Fig. 8. As shown in Fig. 8(d), the requirement on high FD approximation accuracy at $d = 1$ is fulfilled. When $d = 0.5$, the frequency response error is bounded to the

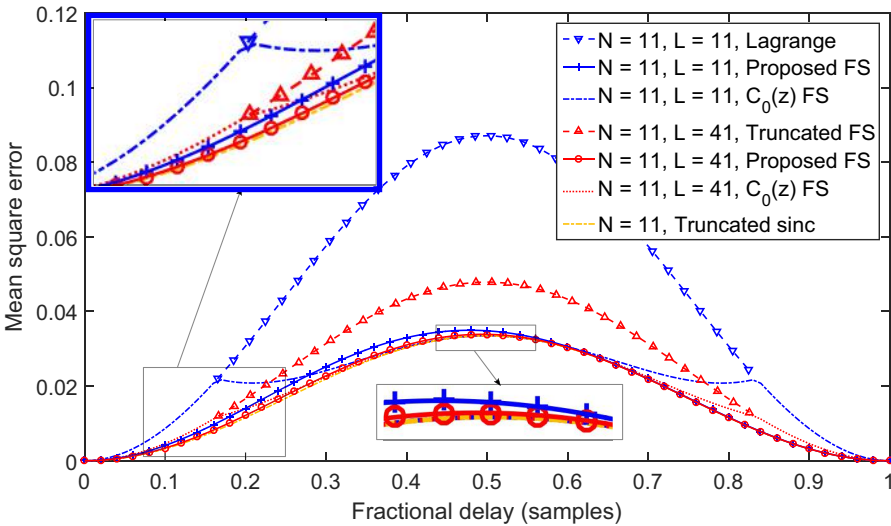


Fig. 7. MSE curves of proposed filter structure of order $N = 11$ and $K = 0$.

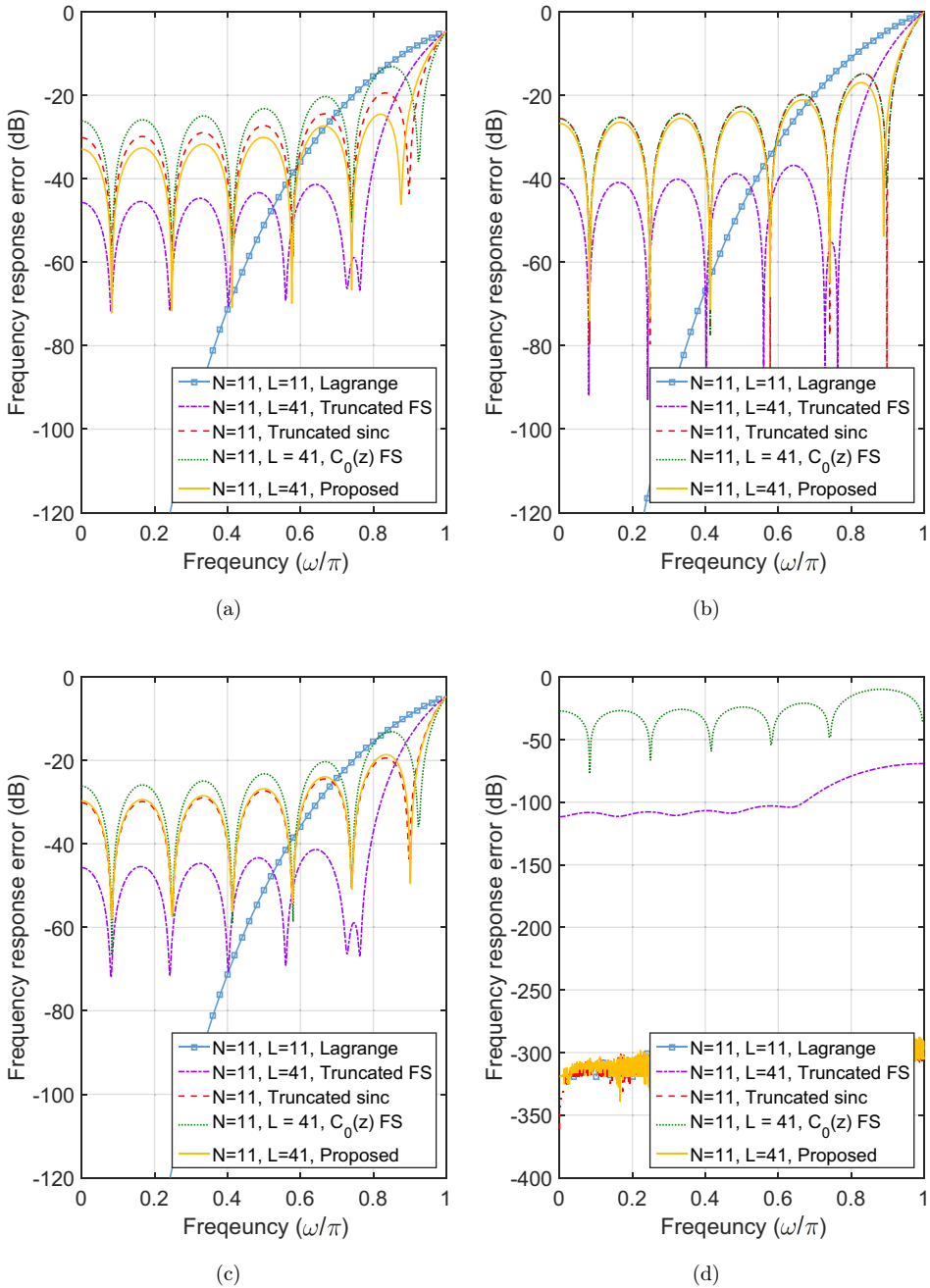


Fig. 8. Frequency response error of different FD interpolation filters at (a) $d = 0.2$, (b) $d = 0.5$, (c) $d = 0.8$ and (d) $d = 1$ with filter orders $(N, K) = (11, 0)$ and parameters $\{m_1, m_2, m_3\} = \{1, 4, 11\}$.

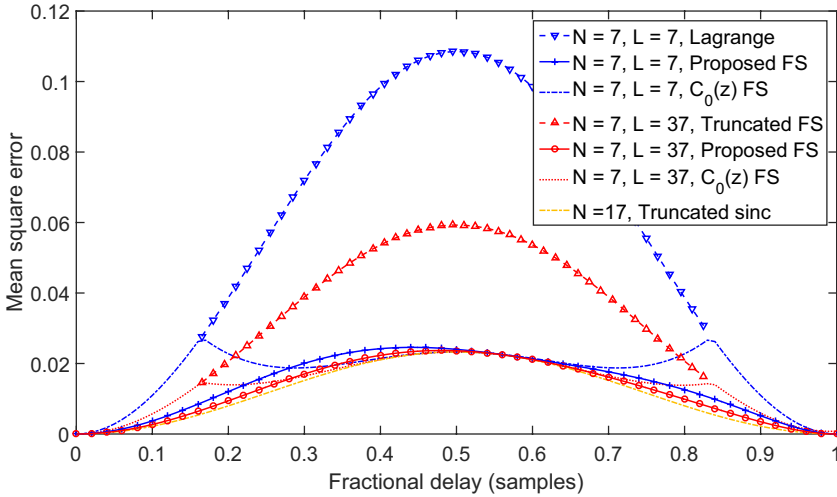


Fig. 9. MSE curves of proposed filter structure with filter order $(N, K) = (7, 5)$ and parameters $\{m_1, m_2, m_3\} = \{1, 4, 7\}$.

error of the truncated *sinc* as shown in Fig. 8(b). Because the maximal flatness is traded-off for the extended bandwidth, the MSE approaches the optimum for a given FD d and filter order N . The MSE performance with optimized filter orders is presented in Fig. 9 and the corresponding frequency response errors are presented in Fig. 10. Note that we do not claim that the resulted combination of filter orders and the set $\{m_1, m_2, m_3\}$ is the optimum one (to this end, one needs to do extra research). The degree of polynomial M and the filter order N ($M = N$ for FS-based Lagrange) are decreased and the filter order of the correction term $N + 2K$ is increased, leading to improvements in FD approximation: less passband ripple, more bandwidth and low MSE level over the entire FD range. In Fig. 10(a), the “ $C_0(z)$ FS” interpolation filter has notable degradation at $d = 0.2$ compared to the proposed filter. At $d = 0.5$, the difference among truncated *sinc* “ $C_0(z)$ FS” and the proposed filters is negligible since both “ $C_0(z)$ FS” and the proposed filters are corrected by introducing the truncated *sinc* of $d = 0.5$ as correction term into their FSs.

4.4. Relation to Lagrange interpolation and combined filter

The impact of these correction terms to the overall impulse response of Lagrange interpolation is given by

$$\Delta g(n, d) = \Delta h_{m_1}(n)d^{m_1} + \Delta h_{m_2}(n)d^{m_2} + \Delta h_{m_3}(n)d^{m_3}, \quad 0 \leq n \leq N. \quad (23)$$

The proposed interpolation filter is more accurate in the LS error sense than the Lagrange interpolation by introducing the truncated *sinc* as correction terms into the FS. The proposed method also provides other optimization parameters

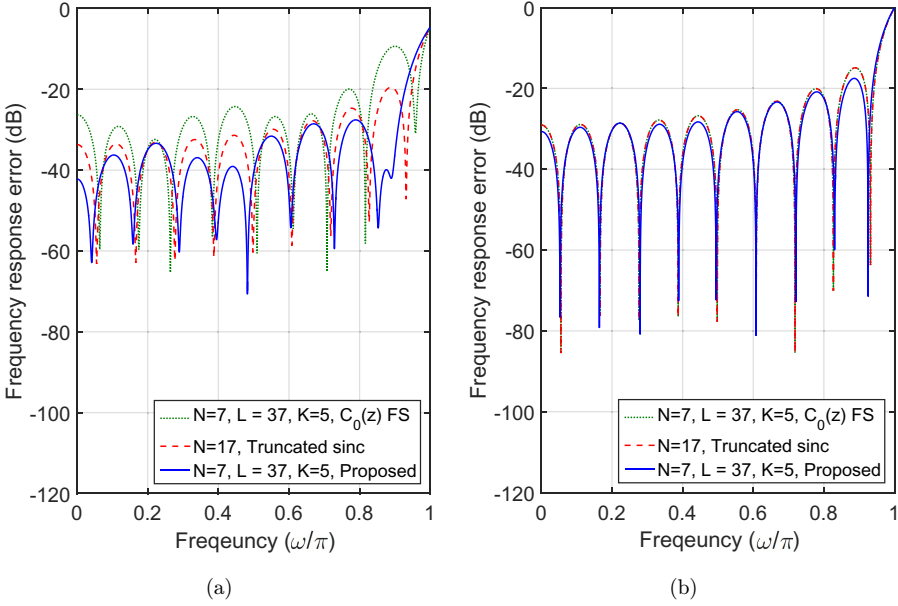


Fig. 10. Frequency response error of different FD interpolation filters with optimized filter orders $(N, K) = (7, 5)$ and parameters $\{m_1, m_2, m_3\} = \{1, 4, 7\}$ at (a) $d = 0.2$ and (b) $d = 0.5$.

$\{m_1, m_2, m_3\}$. By carefully choosing these parameters, the maximal flatness can be traded-off for lower MSEs or more bandwidth in the magnitude response and group delay as shown in Fig. 11. When $\omega_p < \pi$, a new optimal FD interpolation filter can be obtained using the LS design criterion and similar design techniques can be applied to trade-off the maximal flatness in Lagrange for lower MSE. However, it should be pointed out that, for $\omega_p < \pi$, the (truncated) Lagrange FD interpolation has better performance than in the all-pass case, since the FD interpolation degradation at high frequencies can be located in the “don’t care band” specified by $[\omega_p, \pi]$. Compared to the cascaded or the combined filter, the burdensome switching between different filters is removed in the proposed filter structure. Besides, a superior performance is achieved in the LS sense when d is close to 0 or 1. Moreover, the proposed filter approaches the optimal MSE for all variable FDs, however, as mentioned in Sec. 2.1, the truncated *sinc* $\hat{h}(n)$ is only optimal for a given d , and hence for variable d , a new FD interpolation filter has to be implemented each time.

4.5. Implementation cost

The computational cost of FS-based Lagrange with filter order N is $N(N + 1) + N$ multiplications and $N^2 + N$ additions per output sample. Note that $C_0(z)$ is equal to 1 for all delay values in the original FS. Thus, the implementation cost of $C_0(z)$ is discarded. In Table 1, the computational complexity of different implementations is

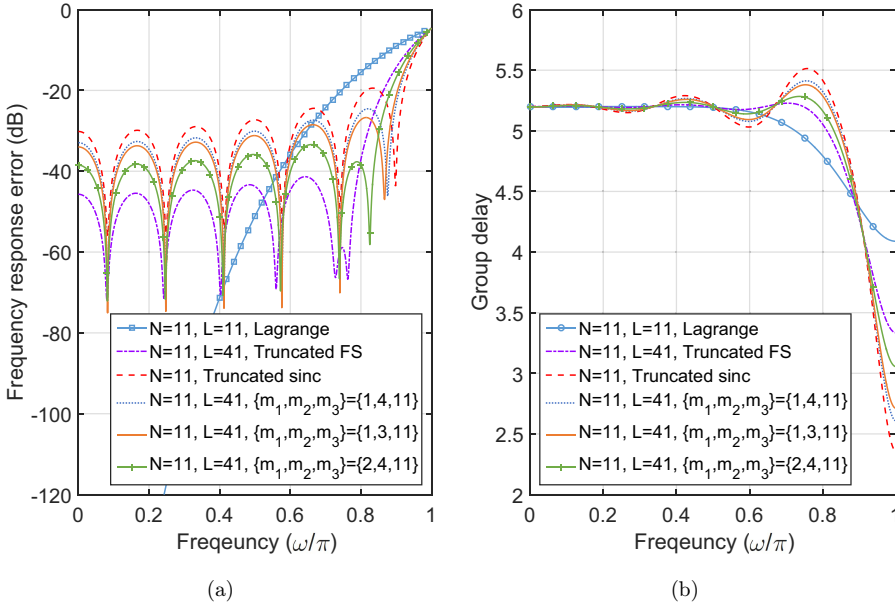


Fig. 11. Frequency response error and group delay of different sets of $\{m_1, m_2, m_3\}$. The filter order $\{N, K, L\} = \{11, 0, 41\}$ and $d = 0.2$ are used.

Table 1. Computational complexity comparison for the combined filter and the proposed structure, only counting the number of multipliers and adders.

	$C_0(z)$ FS structure (N, K) = (11, 0)	Proposed structure (N, K) = (11, 0)	$C_0(z)$ FS structure (N, K) = (7, 5)	Proposed structure (N, K) = (7, 5)
	Mul + Add	Mul + Add	Mul + Add	Mul + Add
$\Delta H(z)$	12 + 11	0 + 0	18 + 17	30 + 27
Farrow	143 + 132	143 + 132	63 + 56	63 + 56
Total	155 + 143	143 + 132	81 + 73	93 + 100

compared in terms of the number of multiplications (Mul) and additions (Add). These results correspond to Figs. 8 and 9, respectively. $\Delta H(z)$ represents the extra correction term introduced. When $\Delta H(z)$ has the same filter order of the FS with $(N, K) = (11, 0)$, a superior performance is achieved by the proposed filter structure even at lower implementation cost. The implementation cost is quadratically reduced by lowering the order of the FS. In addition, the constant coefficient multiplication in the FS can be efficiently implemented on FPGA without dedicated multipliers (e.g., DSP48), instead, only a limited number of shifters and adders are required by using the CSD representation. The utilization of the CSD representation can dramatically reduce the number of nonzero bits representing the constant coefficient, therefore reducing the amount of calculation.

5. Conclusion

This paper has proposed a maximally flat and LS co-design method of a variable FD interpolation filter. This method introduces the truncated *sinc* as correction terms into the FS of a Lagrange interpolation filter. It has been shown that the proposed structure not only features the advantages of the pipelined FS in terms of variable FD interpolation and high throughput, but also enhances the FD approximation. It is shown in the example designs that an overall MSE of approximately 2% is achieved at lower implementation cost with the proposed structure compared to 4% MSE with a traditional implementation. The considerably lower level of MSE over the whole FD range implies that this proposed structure outperforms both the truncated Lagrange interpolation with an FS and the cascaded or combined structure. These features are beneficial to real-time FPGA implementation for sample rate conversion, digital beamforming and symbol synchronization in wideband SDR systems.

Acknowledgments

A preliminary version of this paper has been presented at the 2017 40th International Conference on Telecommunications and Signal Processing (TSP).³⁰ Piet Demeester thanks the ERC for his advanced Grant 695495 ATTO: A new concept for ultra-high capacity wireless networks.

References

1. Y. X. Zou, S. L. Zhang, Y. C. Lim and X. Chen, Timing mismatch compensation in time-interleaved ADCs based on multichannel Lagrange polynomial interpolation, *IEEE Trans. Instrum. Meas.* **60** (2011) 1123–1131.
2. K. M. Tsui and S. C. Chan, New iterative framework for frequency response mismatch correction in time-interleaved ADCs: Design and performance analysis, *IEEE Trans. Instrum. Meas.* **60** (2011) 3792–3805.
3. C. A. Schmidt, J. E. Cousseau, J. L. Figueroa, B. T. Reyes and M. R. Hueda, Efficient estimation and correction of mismatch errors in time-interleaved ADCs, *IEEE Trans. Instrum. Meas.* **65** (2016) 243–254.
4. A. Franck, Efficient algorithms for arbitrary sample rate conversion with application to wave field synthesis, PhD dissertation, Technical University Ilmenau, Germany (2011).
5. A. Aggarwal, M. Kumar, T. K. Rawat and D. K. Upadhyay, Optimal design of 2D FIR filters with quadrantly symmetric properties using fractional derivative constraints, *Circuits Syst. Signal Process.* **35** (2016) 2213–2257.
6. M. Guo, X. Ma, S. Zhang and W. Sheng, The FPGA implementation and verification of variable fractional delay broadband beamforming, *2016 IEEE Int. Workshop on Electromagnetics: Applications and Student Innovation Competition (iWEM)* (IEEE, Nanjing, China, 2016), pp. 1–3.
7. M. T. Shiue and C. L. Wey, Efficient implementation of interpolation technique for symbol timing recovery in DVB-T transceiver design, *Proc. IEEE Int. Conf. Electro/Information Technology* (IEEE, East Lansing, USA, 2006), pp. 427–431.

8. L. Erup, F. M. Gardner and R. A. Harris, Interpolation in digital modems-part II: Implementation and performance, *IEEE Trans. Commun.* **41** (1993) 998–1008.
9. V. Välimäki, Discrete-time modeling of acoustic tubes using fractional delay filters, PhD dissertation, Helsinki University of Technology, Espoo, Finland (1995).
10. C. W. Farrow, A continuously variable digital delay element, *Proc. IEEE Int. Symp. Circuits Systems* (IEEE, Espoo, Finland, 1988), pp. 2641–2645.
11. J. Vesma and T. Saramäki, Optimization and efficient implementation of FIR filters with adjustable fractional delay, *Proc. IEEE Int. Symp. Circuits and Systems* (IEEE, Hong Kong, 1997), pp. 2256–2259.
12. J. Vesma, Optimization and applications of polynomial-based interpolation filters, PhD dissertation, Tampere University of Technology, Tampere, Finland (1999).
13. H. Johansson and P. Löwenborg, On the design of adjustable fractional delay FIR filters, *IEEE Trans. Circuits Syst. II, Analog Digit. Signal Process.* **50** (2003) 164–169.
14. M. Abbas, O. Gustafsson and H. Johansson, On the fixed-point implementation of fractional-delay filters based on the Farrow structure, *IEEE Trans. Circuits Syst. I, Reg. Papers* **60** (2013) 926–937.
15. C. K. S. Pun, Y. C. Wu, S. C. Chan and K. L. Ho, On the design and efficient implementation of the Farrow structure, *IEEE Signal Process. Lett.* **10** (2003) 189–192.
16. K. Khamei, A. Nabavi, S. Hessabi and S. A. M. Barandagh, Design of variable fractional delay FIR filters with CSD coefficients using genetic algorithm, *J. Circuits Syst. Comput.* **14** (2005) 1145–1155.
17. H. Johansson and E. Hermanowicz, Two-rate based low-complexity variable fractional-delay FIR filter structures, *IEEE Trans. Circuits Syst. I, Reg. Papers* **60** (2013) 136–149.
18. C. C. Tseng and S. L. Lee, Design of wideband fractional delay filters using derivative sampling method, *IEEE Trans. Circuits Syst. I, Reg. Papers* **57** (2010) 2087–2098.
19. T. B. Deng and Y. Lian, Weighted-least-squares design of variable fractional-delay FIR filters using coefficient symmetry, *IEEE Trans. Signal Process.* **54** (2006) 3023–3038.
20. Y. D. Huang, S. C. Pei and J. J. Shyu, WLS design of variable fractional-delay FIR filters using coefficient relationship, *IEEE Trans. Circuits Syst. II, Exp. Briefs* **56** (2009) 220–224.
21. M. Kumar and T. K. Rawat, Design of a variable fractional delay filter using comprehensive least square method encompassing all delay values, *J. Circuits Syst. Comput.* **24** (2015) 1550116.
22. M. Kumar and T. K. Rawat, Fractional order digital differentiator design based on power function and least squares, *Int. J. Electron.* **103** (2016) 1639–1653.
23. X. Huang, B. Zhang, H. Qin and W. An, Closed-form design of variable fractional-delay FIR filters with low or middle cutoff frequencies, *IEEE Trans. Circuits Syst. I, Reg. Papers* **65** (2018) 628–637.
24. T. B. Deng, S. Chivapreecha and K. Dejhan, Bi-minimax design of even-order variable fractional-delay FIR digital filters, *IEEE Trans. Circuits Syst. I, Reg. Papers* **59** (2012) 1766–1774.
25. S. Samadi, M. O. Ahmad and M. N. S. Swamy, Results on maximally flat fractional-delay systems, *IEEE Trans. Circuits Syst. I, Reg. Papers* **51** (2004) 2271–2286.
26. S.-C. Pei, P.-H. Wang and H.-S. Lin, Closed-form design of maximally flat FIR fractional delay filters, *IEEE Signal Process. Lett.* **13** (2006) 405–408.
27. T. Laakso, V. Välimäki, M. Karjalainen and U. Laine, Splitting the unit delay, *IEEE Signal Process. Mag.* **13** (1996) 30–60.
28. V. Välimäki and A. Haghparast, Fractional delay filter design based on truncated Lagrange interpolation, *IEEE Signal Process. Lett.* **14** (2007) 816–819.

29. J. Vesma and T. Saramäki, Polynomial-based interpolation filters-part I: Filter synthesis, *Circuits Syst. Signal Process.* **26** (2007) 115–146.
30. H. Li, G. Torfs, T. Kazaz, J. Bauwelinck and P. Demeester, Farrow structured variable fractional delay Lagrange filters with improved midpoint response, *2017 40th Int. Conf. Telecommunications and Signal Processing (TSP)* (IEEE, Barcelona, Spain, 2017), pp. 506–509.